

The ADER high-order approach for solving evolutionary PDEs

Eleuterio TORO
Laboratory of Applied Mathematics
University of Trento, Italy
www.ing.unitn.it/toro
toro@ing.unitn.it

1

Introduction

I am indebted to many collaborators:

Richard Millington

Mauricio Caceres

Tomas Schwarzkopff

Claus-Dieter Munz

Vladimir Titarev

Yoko Takakura

Michael Dumbser

Martin Kaeser

Cedric Enaux

Cristobal Castro

Giovanni Russo

Carlos Pares

Manuel Castro

Arturo Hidalgo

Gianluca Vignoli

Giovanna Grosso

Matteo Antuono

Alberto Canestrelli

Annunziato Siviglia

Gino Montecinos

Lucas Mueller

Junbo Cheng

.....

.....

**We are interested in developing numerical methods
for approximating
time-dependent partial differential equations of the form**

$$\partial_t Q + A(Q) = S(Q) + D(Q)$$

AIM:
solve to high (arbitrary) accuracy
in space and time

non-linear systems of hyperbolic balance laws
with stiff/non-stiff source terms
in multiple space dimensions on
structured/unstructured meshes
in the frameworks of
Finite Volume and
Discontinuous Galerkin Finite Element
Methods

Two basic design constraints

- **Methods must be conservative**
(because of the Lax-Wendroff theorem, 1960)
- **Methods must be non-linear**
(because of the Godunov theorem, 1959)

The ADER approach

First results for linear equations in:

E. F. Toro, R. C. Millington and L. A. M. Nejad.

Towards Very High–Order Godunov Schemes.

In Godunov Methods: Theory and Applications. Edited Review.

E. F. Toro (Editor), pages 905–937. Kluwer Academic/Plenum Publishers, 2001

Key features of ADER:

High-order non-linear spatial reconstruction

+

high-order Riemann problem

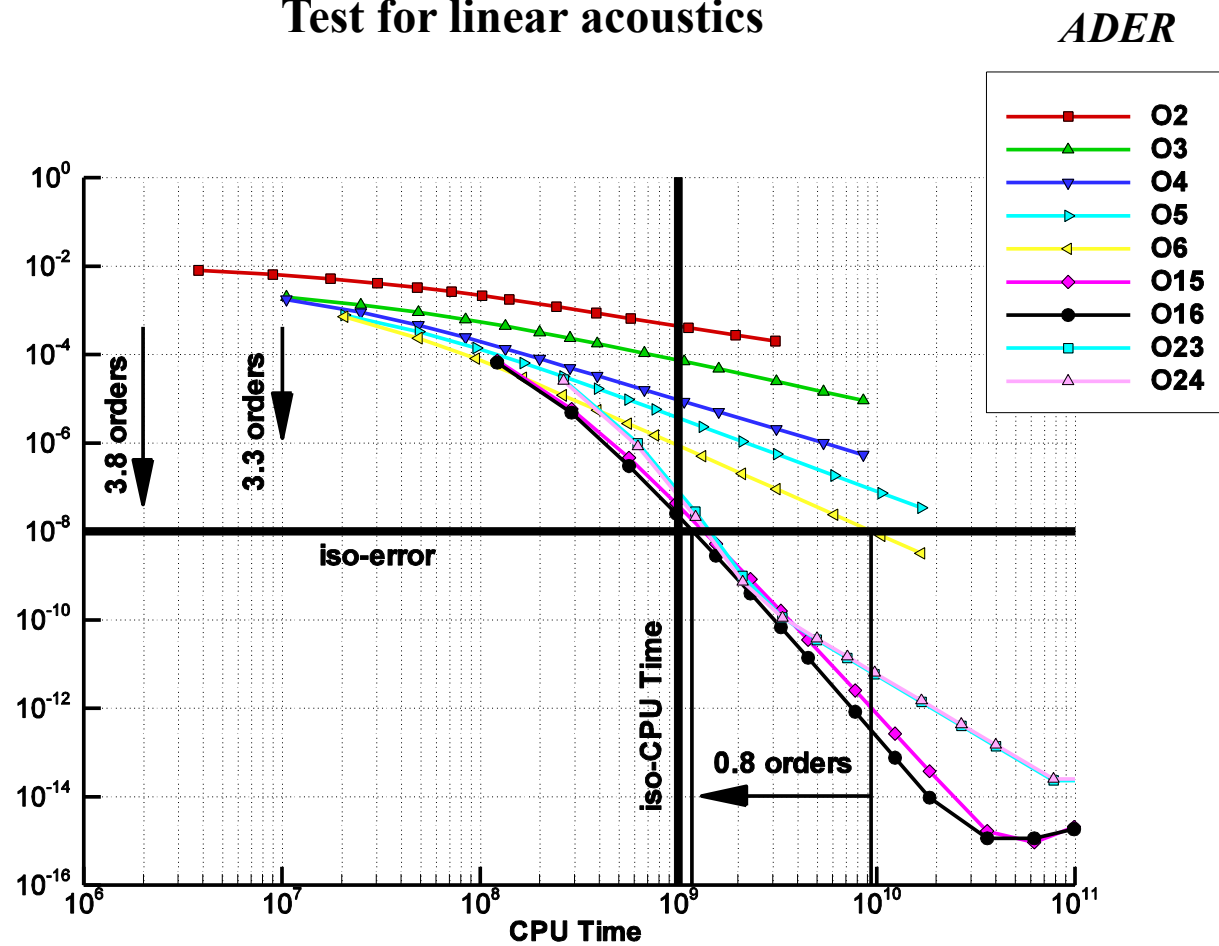
(also called the *Generalized Riemann problem*)

**This *generalized Riemann problem* has initial conditions
with a high-order (spatial) representation, such as polynomials,
and source terms are included**

High accuracy.

But why ?

Test for linear acoustics



Collaborators:

M. Dumbser, T. Schwartzkopff, and C.-D. Munz. **Arbitrary high order finite volume schemes for linear wave propagation.** Book Series Notes on Numerical Fluid mechanics and Multidisciplinary Design. Springer Berlin / Heidelberg
ISSN 1612-2909, Volume 91/2006

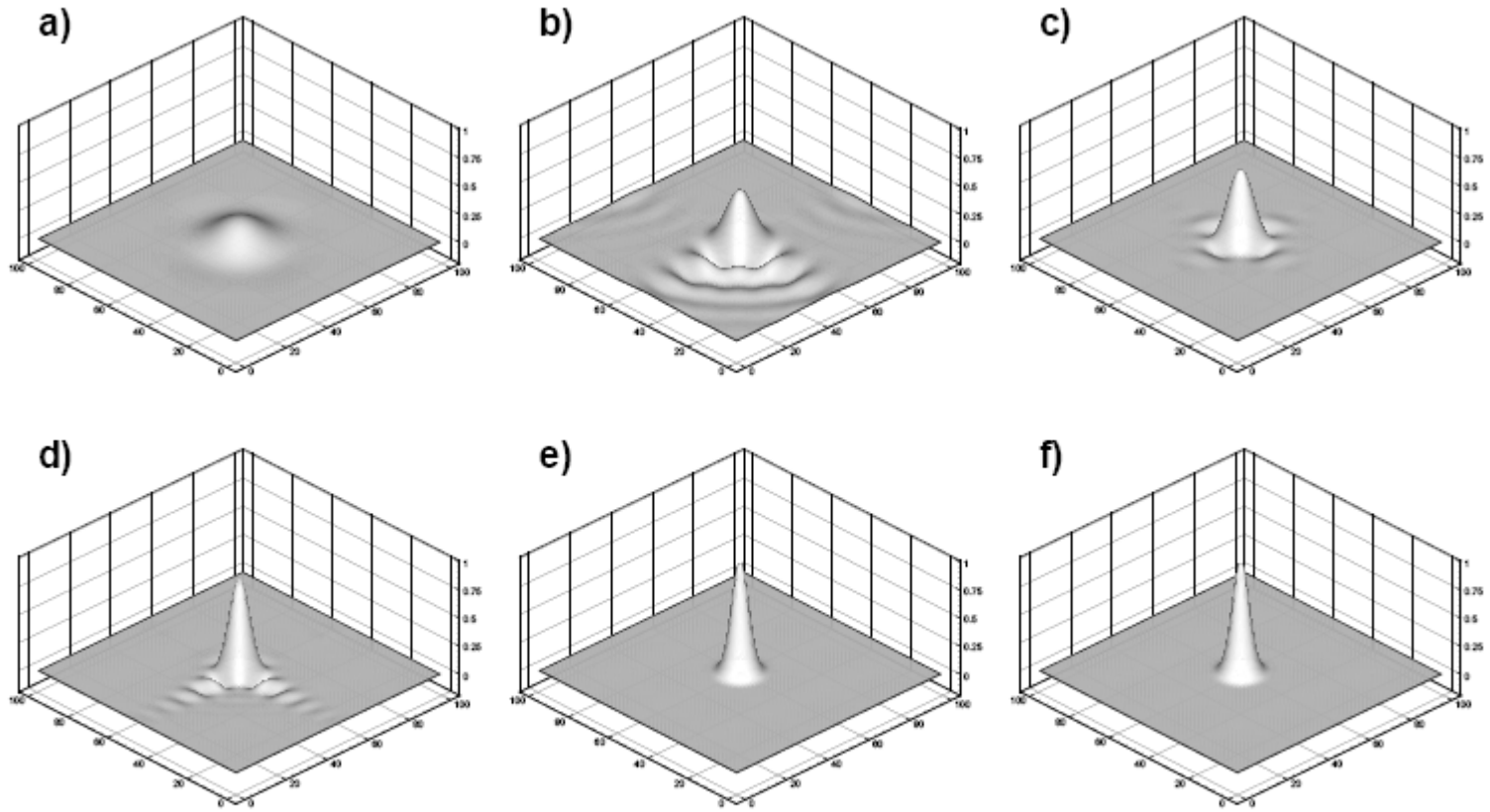


Fig. 4. Gaussian fluctuation with halfwidth of $\sigma = 3$ units at $T = 10000$. a) ADER $\mathcal{O}3$, b) ADER $\mathcal{O}4$, c) ADER $\mathcal{O}5$, d) ADER $\mathcal{O}6$, e) ADER $\mathcal{O}15$, f) ADER $\mathcal{O}16$

2

ADER in 1D

Finite volume formulation

Exact relation between integral averages

$$\partial_t Q + \partial_x F(Q) = S(Q)$$

Integration in space and time
on control volume

$$[x_{i-1/2}, x_{i+1/2}] \times [0, \Delta t]$$

$$Q_i^{n+1} = Q_i^n - \frac{\Delta t}{\Delta x} [F_{i+1/2} - F_{i-1/2}] + \Delta t S_i \quad \text{Exact relation}$$

$$\left. \begin{aligned} Q_i^n &= \frac{1}{\Delta x} \int_{x_{i-1/2}}^{x_{i+1/2}} Q(x, 0) dx \\ F_{i+1/2} &= \frac{1}{\Delta t} \int_0^{\Delta t} F(Q_{i+1/2}(\tau)) d\tau \\ S_i &= \frac{1}{\Delta t} \frac{1}{\Delta x} \int_0^{\Delta t} \int_{x_{i-1/2}}^{x_{i+1/2}} S(Q_i(x, t)) dx dt \end{aligned} \right\} \quad \text{Integral averages}$$

Data reconstruction:

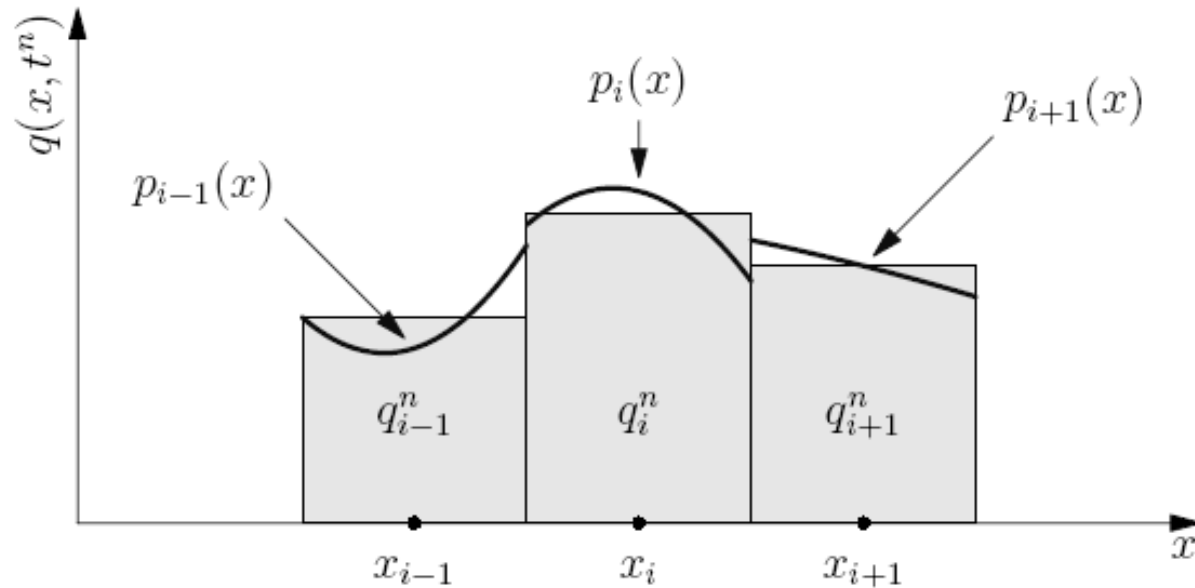
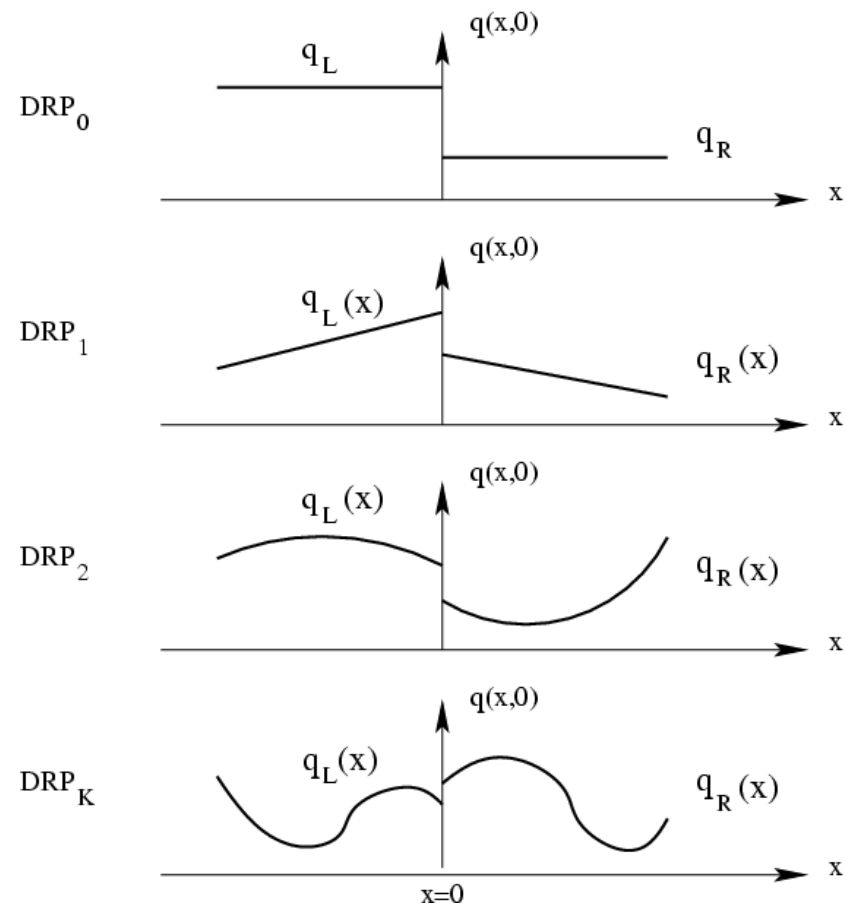


Fig. 20.1. Cell averages $\{q_i^n\}$ define a piece-wise constant distribution $\{p_i(x)\}$ on each cell i . Illustration of reconstructed polynomial functions $p_{i-1}(x)$, $p_i(x)$ and $p_{i+1}(x)$ in cells $i - 1$, i and $i + 1$, respectively.

M. Dumbser, M. Kaser, V. A. Titarev, and E. F. Toro. Quadrature-Free Non-Oscillatory Finite Volume Schemes on Unstructured Meshes for Nonlinear Hyperbolic Systems. J. Comput. Phys., 226(8):204–243, 2007.

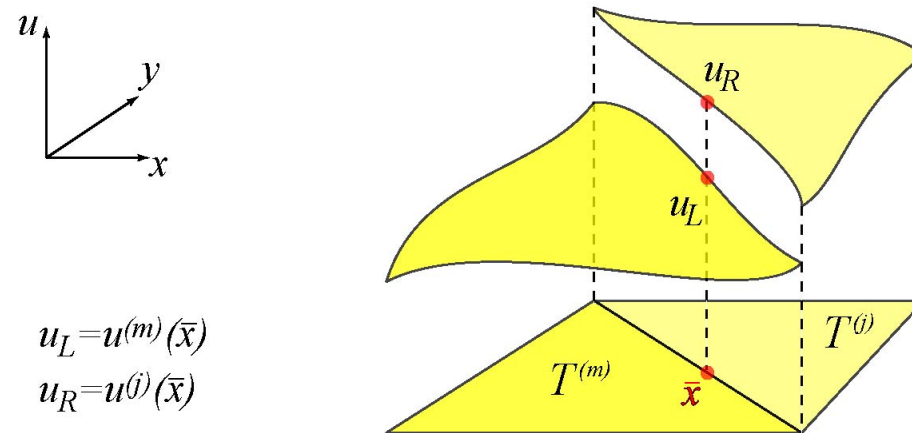
Data variation across interface



In 3D

$$\partial_t \mathbf{Q} + \partial_x \mathbf{F}(\mathbf{Q}) + \partial_y \mathbf{G}(\mathbf{Q}) + \partial_z \mathbf{H}(\mathbf{Q}) = \mathbf{S}(\mathbf{Q})$$

$$\mathcal{H}_{i+\frac{1}{2}} = \frac{1}{\Delta t} \int_{t_n}^{t_{n+1}} \left(\int \int_{A_k} \mathcal{H} \cdot \mathbf{n}_k dA \right) dt$$



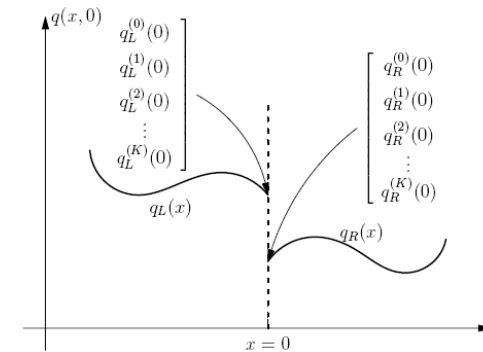
The numerical flux requires the calculation of an integral in space along the volume/element interface and in time.

A key ingredient:

the high-order
(or generalized)
Riemann problem

The high-order (or generalized) Riemann problem:

$$\left. \begin{aligned} &\partial_t Q + \partial_x F(Q) = S(Q) \\ &Q(x,0) = \begin{cases} Q_L(x) & \text{if } x < 0 \\ Q_R(x) & \text{if } x > 0 \end{cases} \end{aligned} \right\} \text{GRP}_K$$



Initial conditions: two smooth functions

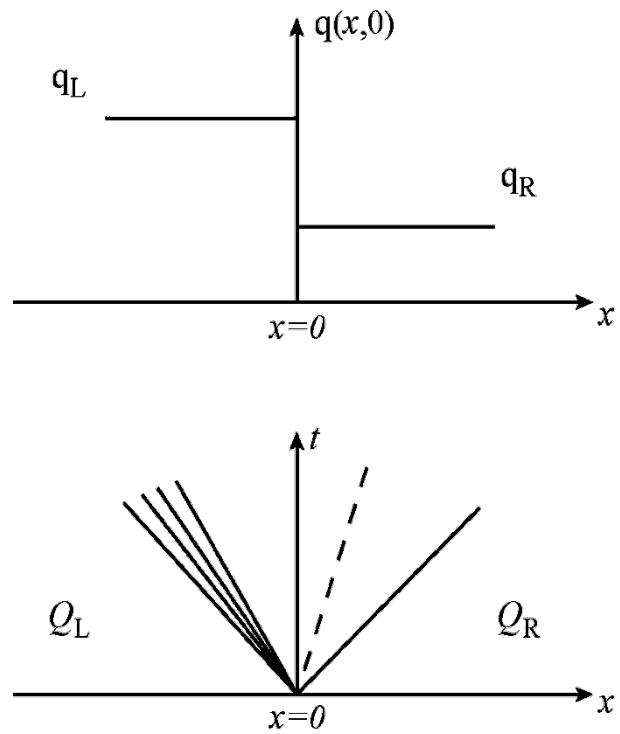
$$Q_L(x), Q_R(x)$$

For example, two polynomials of degree K

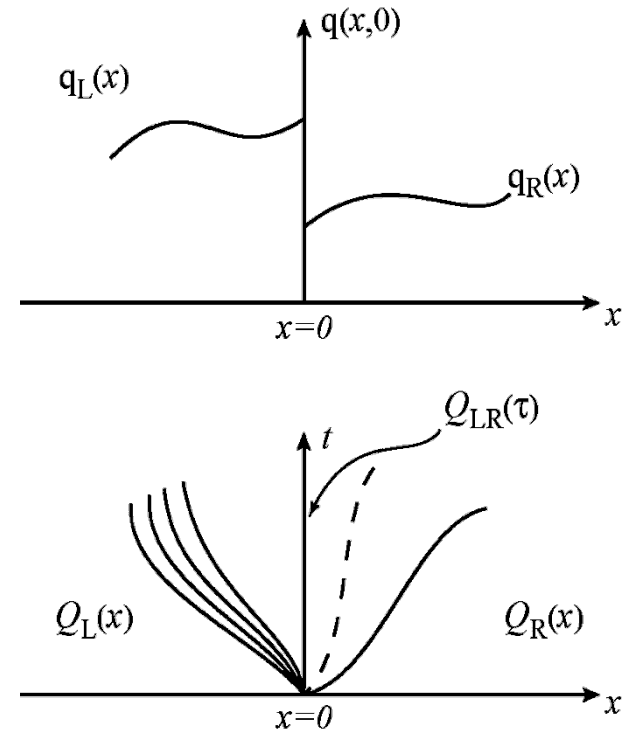
The generalization is twofold:

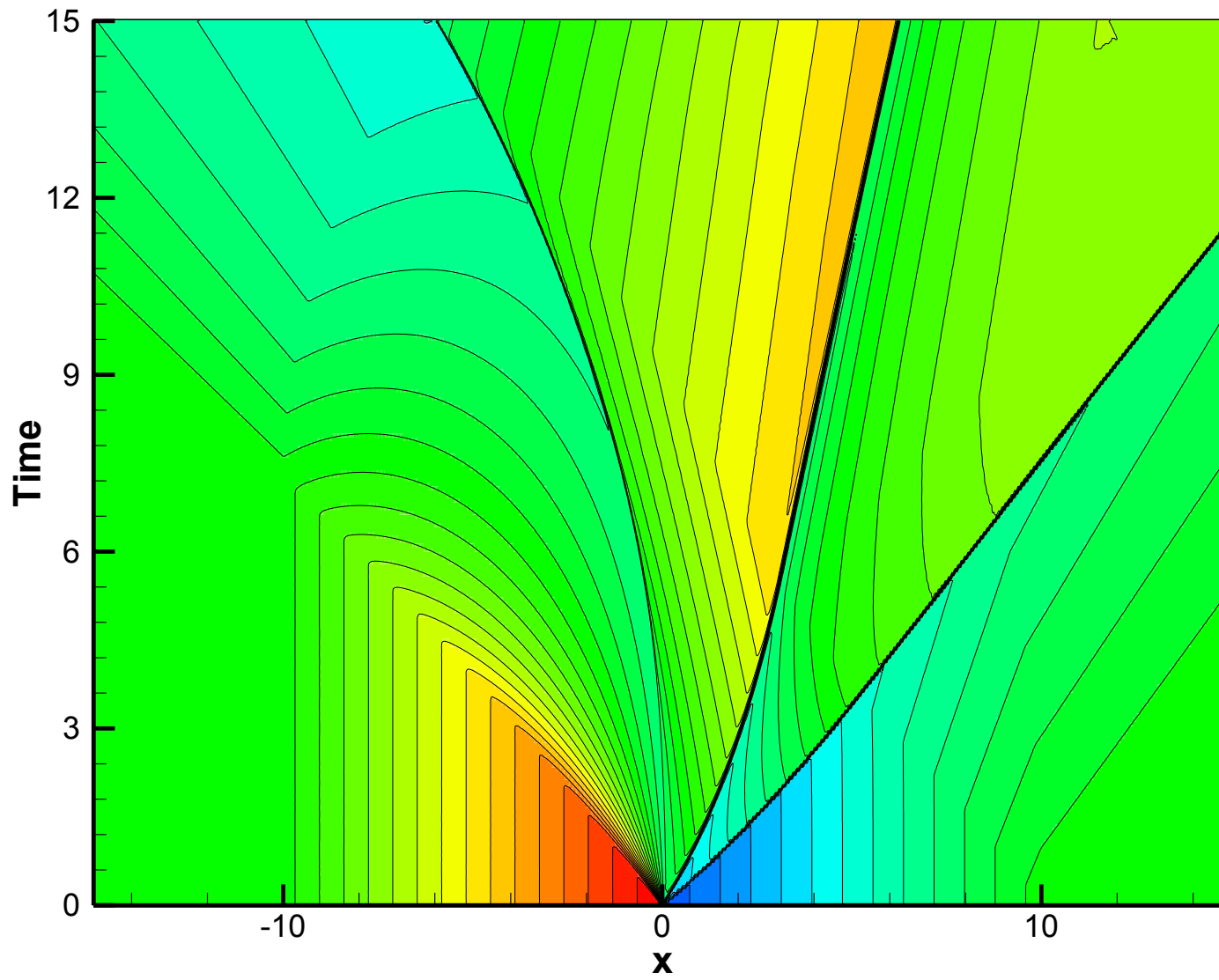
- (1) the initial conditions are two polynomials of arbitrary degree
- (2) the equations include source terms

Classical Riemann Problem



Derivative Riemann Problem





3

*A solver for the
generalized Riemann problem*

$$Q_{LR}(\tau) = Q(0,0_+) + \sum_{k=1}^K \partial_t^{(k)} Q(0,0_+) \frac{\tau^k}{k!}$$

$$Q(0,0_+) = \lim_{t \rightarrow 0_+} Q(0,t)$$

Extension of work of Ben-Artzi and Falcovitz, 1984, see also Raviart and LeFloch 1989

See also the related work of Harten et al, 1987.

**The leading term
and
higher-order terms**

E. F. Toro and V. A. Titarev. Solution of the Generalised Riemann Problem for Advection–Reaction Equations. *Proc. Roy. Soc. London A*, 458:271–281, 2002.

E. F. Toro and Titarev V. A. Derivative Riemann Solvers for Systems of Conservation Laws and ADER Methods. *J. Comput. Phys.*, 212(1):150–165, 2006.

Available information at time $t=0$

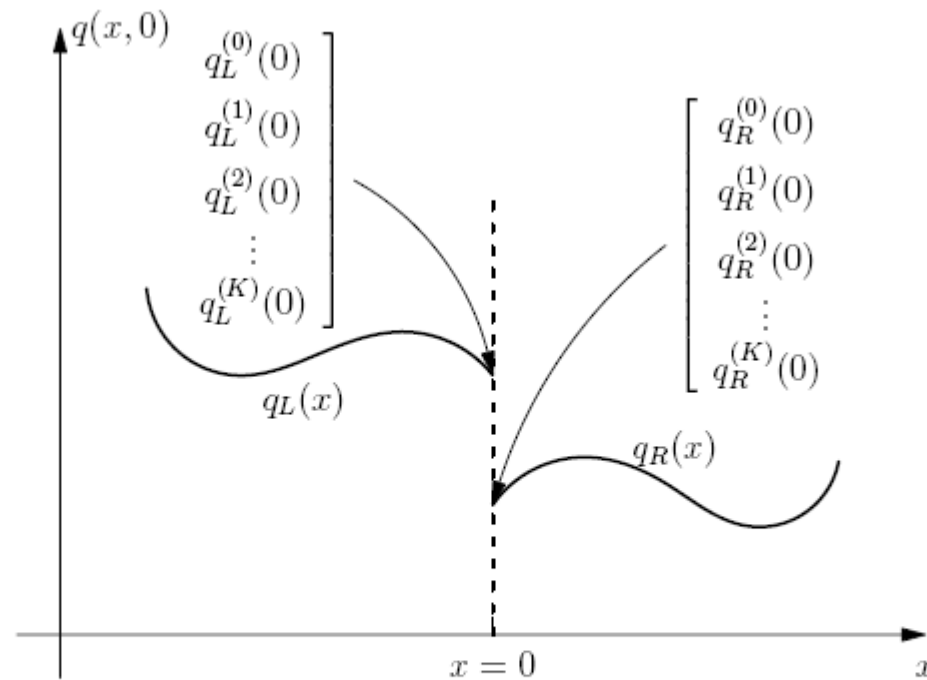


Fig. 19.3. Illustration of the initial conditions for the generalized Riemann problem GRP_K for a single component $q(x, t)$ of the vector of unknowns $\mathbf{Q}(x, t)$. The data $q_L(x)$ and $q_R(x)$ are smooth functions away from $x = 0$ and have one-sided spatial derivatives at $x = 0$.

Computing the leading term in

$$Q_{LR}(\tau) = Q(0,0_+) + \sum_{k=1}^K \partial_t^{(k)} Q(0,0_+) \frac{\tau^k}{k!}$$

Solve the *classical* RP

$$\left. \begin{aligned} \partial_t \mathbf{Q} + \partial_x \mathbf{F}(\mathbf{Q}) &= \mathbf{0} , \\ \mathbf{Q}(x, 0) &= \begin{cases} \mathbf{Q}_L(0) \equiv \lim_{x \rightarrow 0_-} \mathbf{Q}_L(x) & \text{if } x < 0 , \\ \mathbf{Q}_R(0) \equiv \lim_{x \rightarrow 0_+} \mathbf{Q}_R(x) & \text{if } x > 0 . \end{cases} \end{aligned} \right\}$$

Solution: $D^{(0)}(x/t)$

Take Godunov state at $x/t=0$

Leading term: $Q(0,0_+) = D^{(0)}(0)$

Computing the higher-order terms:

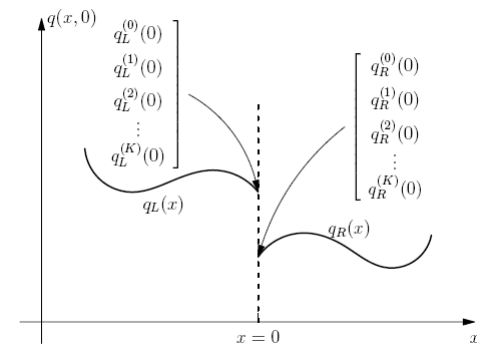
$$Q_{LR}(\tau) = Q(0,0_+) + \sum_{k=1}^K \partial_t^{(k)} Q(0,0_+) \frac{\tau^k}{k!}$$

First use the **Cauchy-Kowalewski (*)** procedure

$$\partial_t^{(k)} Q(x, t) = G^{(k)}(\partial_x^{(0)} Q, \dots, \partial_x^{(k)} Q)$$

Example:

$$\partial_t q + \lambda \partial_x q = 0 \Rightarrow \begin{cases} \partial_t q = -\lambda \partial_x q \\ \partial_t^{(2)} q = (-\lambda)^2 \partial_x^{(2)} q \\ \partial_t^{(m)} q = (-\lambda)^m \partial_x^{(m)} q \end{cases}$$



Must define spatial derivatives at $x=0$ for $t>0$

(*) **Cauchy-Kowalewski theorem.** One of the most fundamental results in the theory of PDEs.
Applies to problems in which all functions involved are analytic.

Computing the higher-order terms...cont..

$$Q_{LR}(\tau) = Q(0,0_+) + \sum_{k=1}^K \partial_t^{(k)} Q(0,0_+) \frac{\tau^k}{k!}$$

Then construct evolution equations for the variables:

$$\partial_x^{(k)} Q(x, t)$$

Note:

$$\partial_t q + \lambda \partial_x q = 0 \Rightarrow \partial_t (\partial_x q) + \lambda \partial_x (\partial_x q) = 0$$

For the general case it can be shown that:

$$\partial_t (\partial_x^{(k)} Q) + A(Q) \partial_x (\partial_x^{(k)} Q) = H^{(k)} (\partial_x^{(0)} Q, \partial_x^{(1)} Q, \dots, \partial_x^{(k)} Q)$$

Neglecting *source terms* and linearizing we have

$$\partial_t (\partial_x^{(k)} Q) + A(Q(0,0_+)) \partial_x (\partial_x^{(k)} Q) = 0$$

Computing the higher-order terms...cont..

$$Q_{LR}(\tau) = Q(0,0_+) + \sum_{k=1}^K \partial_t^{(k)} Q(0,0_+) \frac{\tau^k}{k!}$$

For each k solve *classical* Riemann problem:

$$\left. \begin{aligned} \partial_t (\partial_x^{(k)} Q) + A(Q(0,0_+)) \partial_x (\partial_x^{(k)} Q) &= 0 \\ \partial_x^{(k)} Q(x,0) &= \begin{cases} \partial_x^{(k)} Q_L(0) & \text{if } x < 0 \\ \partial_x^{(k)} Q_R(0) & \text{if } x > 0 \end{cases} \end{aligned} \right\} \text{sol} : D^{(k)}(x/t)$$

Evaluate solution at $x/t=0$

All spatial derivatives at $x=0$ are now defined

$$\partial_x^{(k)} Q(0,0_+) = D^{(k)}(0)$$

Computing the higher-order terms...cont..

$$Q_{LR}(\tau) = Q(0,0_+) + \sum_{k=1}^K \partial_t^{(k)} Q(0,0_+) \frac{\tau^k}{k!}$$

All time derivatives at $x=0$ are then defined

$$\partial_t^{(k)} Q(0,0_+) = G^{(k)}(\partial_x^{(0)} Q(0,0_+), \dots, \partial_x^{(k)} Q(0,0_+))$$

Solution of DRP is:

$$Q_{LR}(\tau) = Q(0,0_+) + \sum_{k=1}^K \partial_t^{(k)} Q(0,0_+) \frac{\tau^k}{k!}$$

GRP-K = 1(non-linear RP) + K (linear RPs)

Options: state expansion and flux expansion

4

Complete ADER scheme

ADER finite volume method for

$$\partial_t Q + \partial_x F(Q) = S(Q)$$

One-step scheme

$$Q_i^{n+1} = Q_i^n - \frac{\Delta t}{\Delta x} [F_{i+1/2} - F_{i-1/2}] + \Delta t S_i$$

Numerical flux:

$$F_{i+1/2} = \frac{1}{\Delta t} \int_0^{\Delta t} F(Q_{i+1/2}(\tau)) d\tau$$

Numerical source:

$$S_i = \frac{1}{\Delta t} \frac{1}{\Delta x} \int_0^{\Delta t} \int_{x_{i-1/2}}^{x_{i+1/2}} S(Q_i(x, t)) dx dt$$

More solvers for the generalized Riemann problem:

C E Castro and E F Toro. Solvers for the high-order Riemann problem for hyperbolic balance laws. Journal Computational Physics Vol. 227, pp 2482-2513, 2008

M Dumbser, C Einaux and E F Toro. Finite volume schemes of very high order of accuracy for stiff hyperbolic balance laws . Journal of Computational Physics, Vol 227, pp 3971-4001, 2008.

Summary of ADER schemes

*one-step
fully discrete schemes for*

$$\partial_t Q + \partial_x F(Q) + \partial_y G(Q) + \partial_z H(Q) = S(Q)$$

Accuracy in space and time is arbitrary

General meshes

Unified framework

Finite volume, DG finite elements

The Cauchy-Kowalewski procedure:

A Fortran Example Code for the Cauchy-Kowalewski Procedure for the 3D Euler Equations

M. Dumbser, M. Käser, V.A. Titarev, E.F. Toro. *Quadrature-free non-oscillatory finite volume schemes on unstructured meshes for nonlinear hyperbolic systems.*
Journal of Computational Physics. Vol. 226, Issue 1, Pages 204-243,
10 September 2007.

How to avoid the Cauchy-Kowalewski procedure:

Numerical evolution of data (related to Harten's method, 1987).

See

M Dumbser, C Enaux and E F Toro. Finite volume schemes of very high order of accuracy for stiff hyperbolic balance laws . Journal of Computational Physics, Vol 227, pp 3971-4001, 2008.

With this solver we can deal with stiff source terms

Work in progress to simplify solvers for the generalized Riemann problem with stiff source terms

Work in progress to simplify solvers for the generalized Riemann problem with stiff source terms

Evaluation/comparison of four currently available generalized Riemann problem solvers:

G I Montecinos, C E Castro, M Dumbser and E F Toro. Comparison of solvers for the generalized Riemann problem for hyperbolic systems with source terms.
Journal of Computational Physics, 2012.
Available on line. DOI: <http://dx.doi.org/10.1016/j.jcp.2012.06.011>

Main applications so far

1, 2, 3D Euler equations on unstructured meshes
3D compressible Navier-Stokes equations
Reaction-diffusion (parabolic equations)
Dispersive systems
Sediment transport in water flows (single phase)
Two-phase sediment transport (Pitman and Le model)
Two-layer shallow water equations
Aeroacoustics in 2 and 3D
Seismic wave propagation in 3D
Tsunami wave propagation
Magnetohydrodynamics
3D Maxwell equations
3D compressible two-phase flow, etc.

5

Sample numerical results

Linear advection

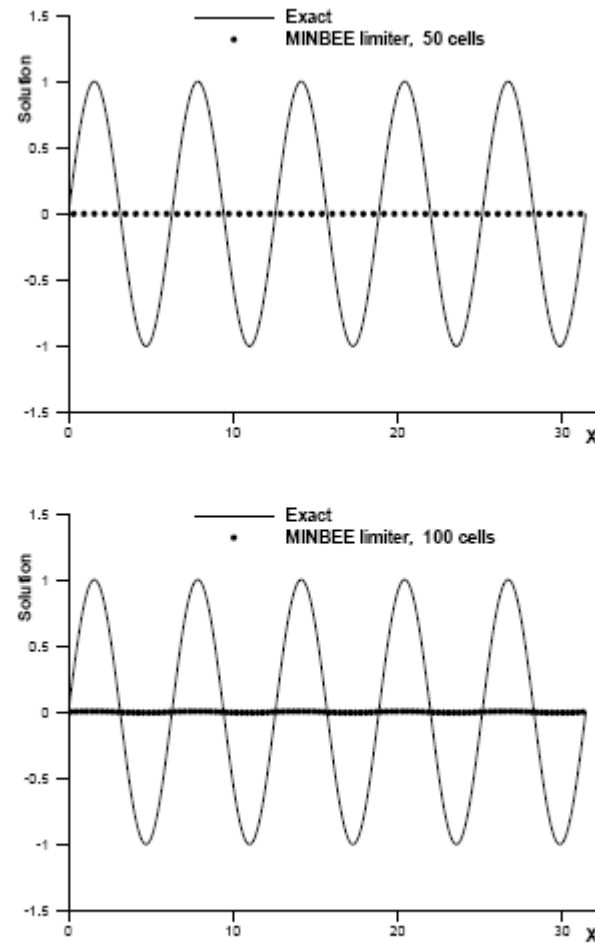


Fig. 20.2. Linear advection. Results from TVD scheme with MINBEE limiter (symbols) at time $t = 1000\pi$ using meshes of 50 and 100 cells, with $C_{eff} = 0.95$. Exact solution shown by full line (Courtesy of Dr. V. A. Titarev).

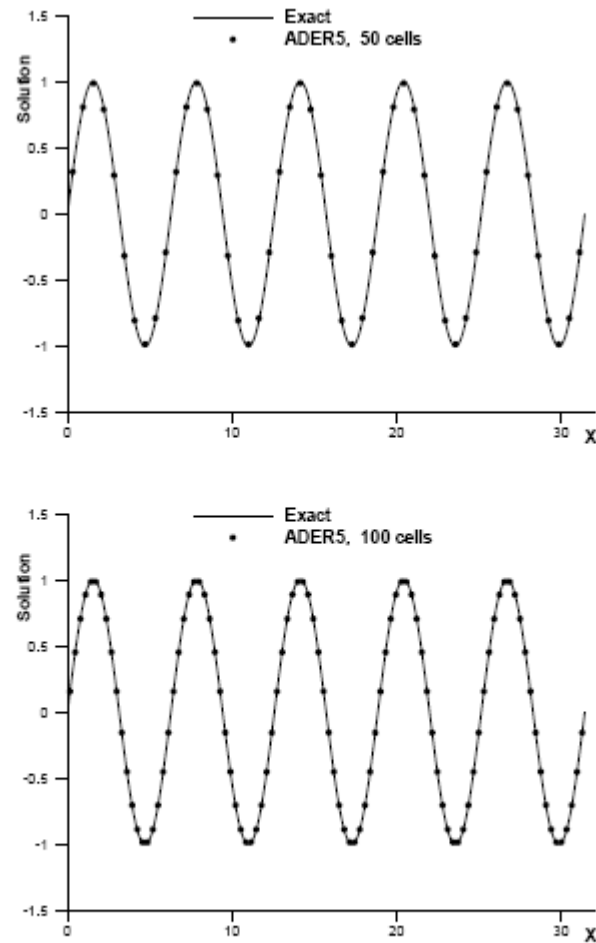
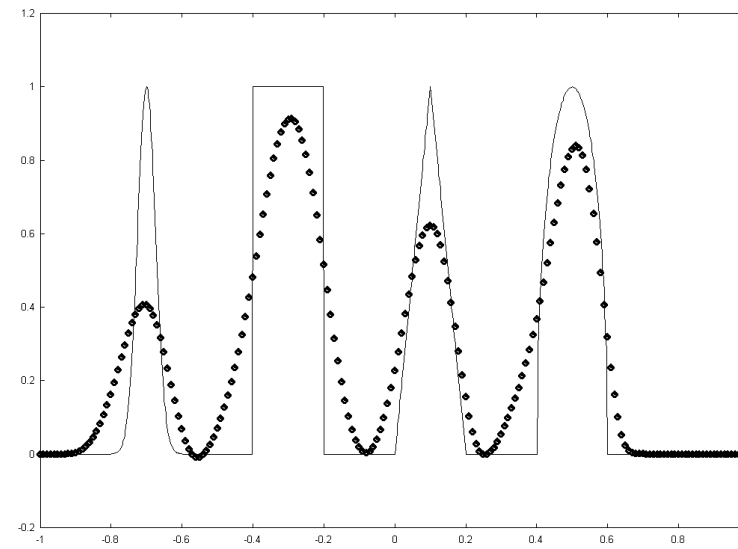
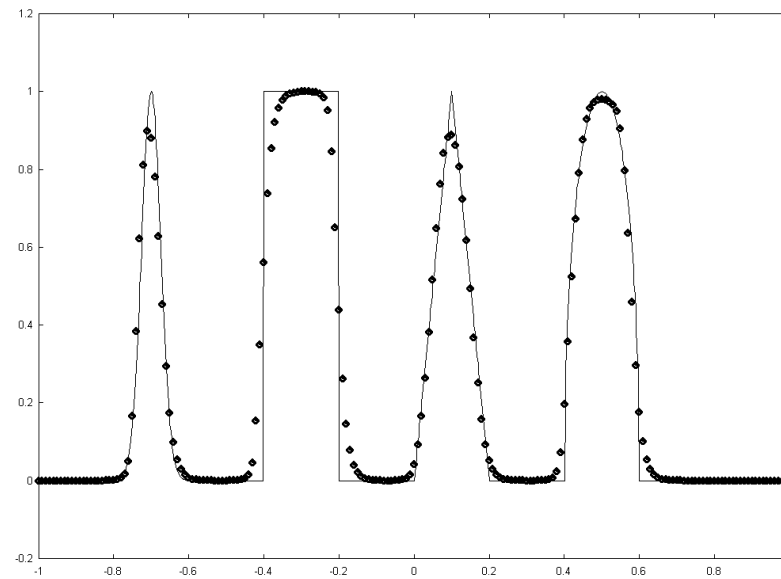


Fig. 20.4. Advection of smooth profile. Results from 5-th order ADER scheme (symbols) at time $t = 1000\pi$ using meshes of 50 and 100 cells, with $C_{cfl} = 0.95$. Exact solution shown by full line (Courtesy of Dr. V. A. Titarev).



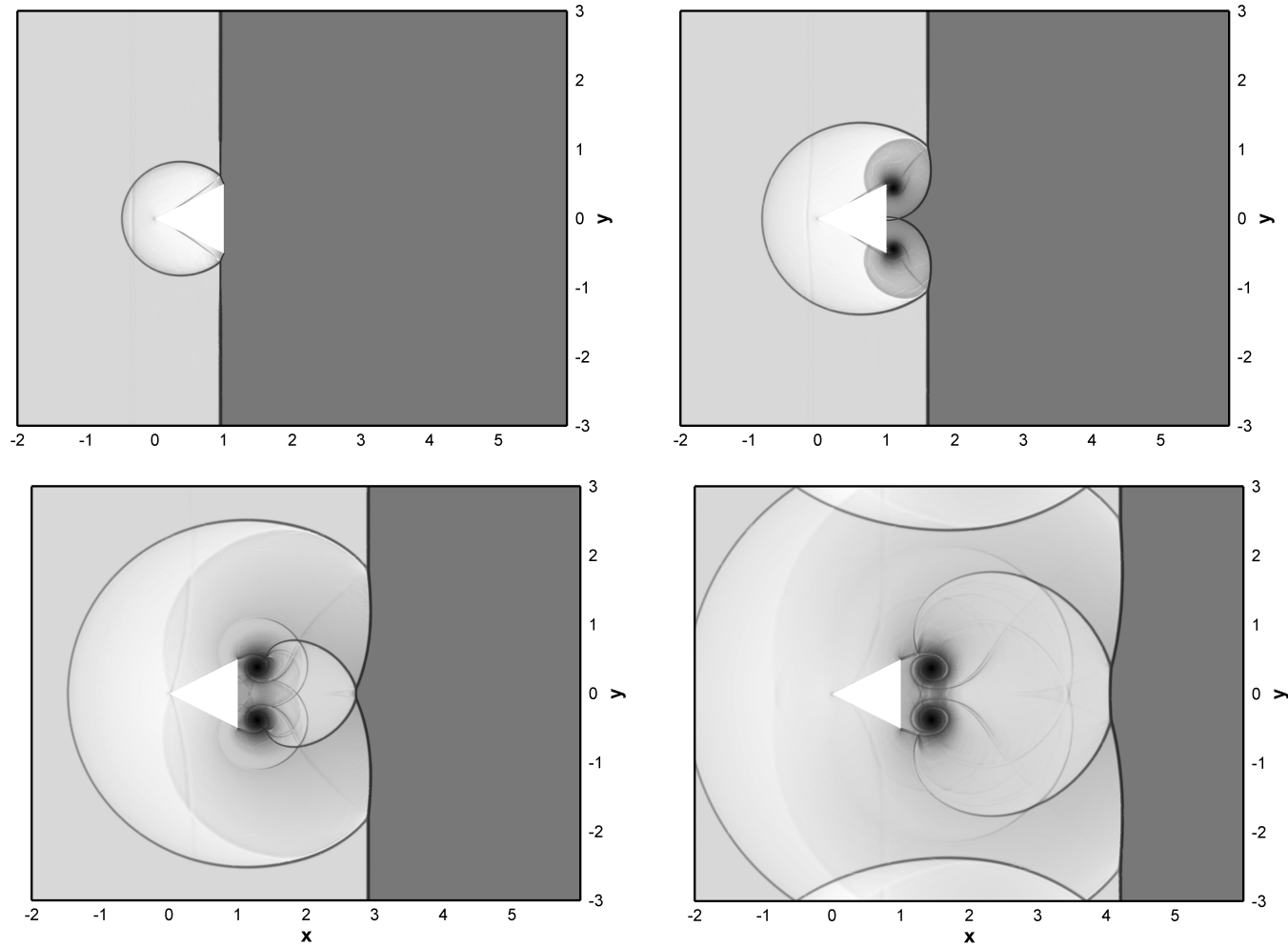
WENO-5



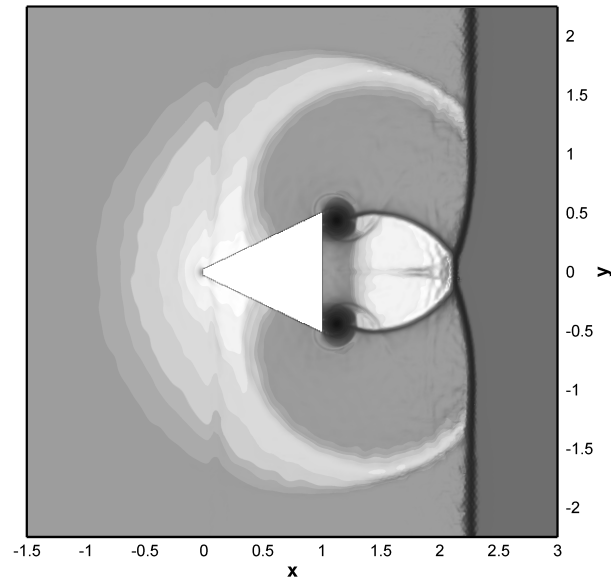
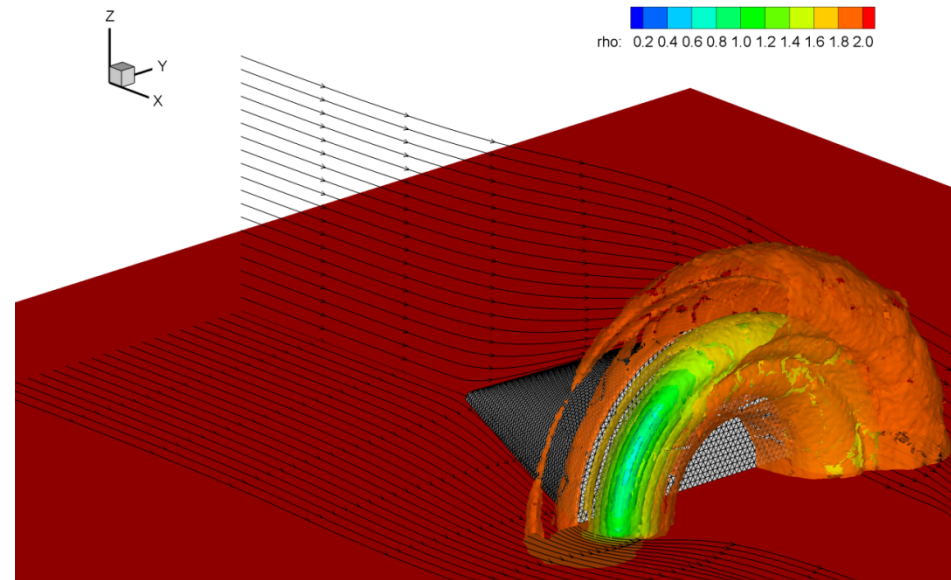
ADER-3

2D and 3D Euler equations

2D Euler equations: reflection from triangular object



3D Euler equations: reflection from cone



2D and 3D Baer-Nunziato equations

3D Baer-Nunziato equations for compressible two-phase flow

$$\left. \begin{aligned}
 &\frac{\partial}{\partial t} (\phi_1 \rho_1) + \nabla \cdot (\phi_1 \rho_1 \mathbf{u}_1) = 0, \\
 &\frac{\partial}{\partial t} (\phi_1 \rho_1 \mathbf{u}_1) + \nabla \cdot (\phi_1 \rho_1 \mathbf{u}_1 \otimes \mathbf{u}_1) + \nabla \phi_1 p_1 = p_I \nabla \phi_1 + \lambda (\mathbf{u}_2 - \mathbf{u}_1), \\
 &\frac{\partial}{\partial t} (\phi_1 \rho_1 E_1) + \nabla \cdot ((\phi_1 \rho_1 E_1 + \phi_1 p_1) \mathbf{u}_1) = -p_I \partial_t \phi_1 + \lambda \mathbf{u}_I \cdot (\mathbf{u}_2 - \mathbf{u}_1), \\
 &\frac{\partial}{\partial t} (\phi_2 \rho_2) + \nabla \cdot (\phi_2 \rho_2 \mathbf{u}_2) = 0, \\
 &\frac{\partial}{\partial t} (\phi_2 \rho_2 \mathbf{u}_2) + \nabla \cdot (\phi_2 \rho_2 \mathbf{u}_2 \otimes \mathbf{u}_2) + \nabla \phi_2 p_2 = p_I \nabla \phi_2 - \lambda (\mathbf{u}_2 - \mathbf{u}_1), \\
 &\frac{\partial}{\partial t} (\phi_2 \rho_2 E_2) + \nabla \cdot ((\phi_2 \rho_2 E_2 + \phi_2 p_2) \mathbf{u}_2) = p_I \partial_t \phi_1 - \lambda \mathbf{u}_I \cdot (\mathbf{u}_2 - \mathbf{u}_1), \\
 &\frac{\partial}{\partial t} \phi_1 + \mathbf{u}_I \nabla \phi_1 = 0.
 \end{aligned} \right\} \quad (54)$$

11 nonlinear hyperbolic PDES

Stiff source terms: relaxation terms

Michael Dumbser, Arturo Hidalgo, Manuel Castro, Carlos Parés and Eleuterio F. Toro
FORCE schemes on unstructured meshes II: Non-conservative hyperbolic systems . Computer methods
in Applied Science and Engineering, Vol. 199, Issues 9-12, pp 625-647, January 2010.

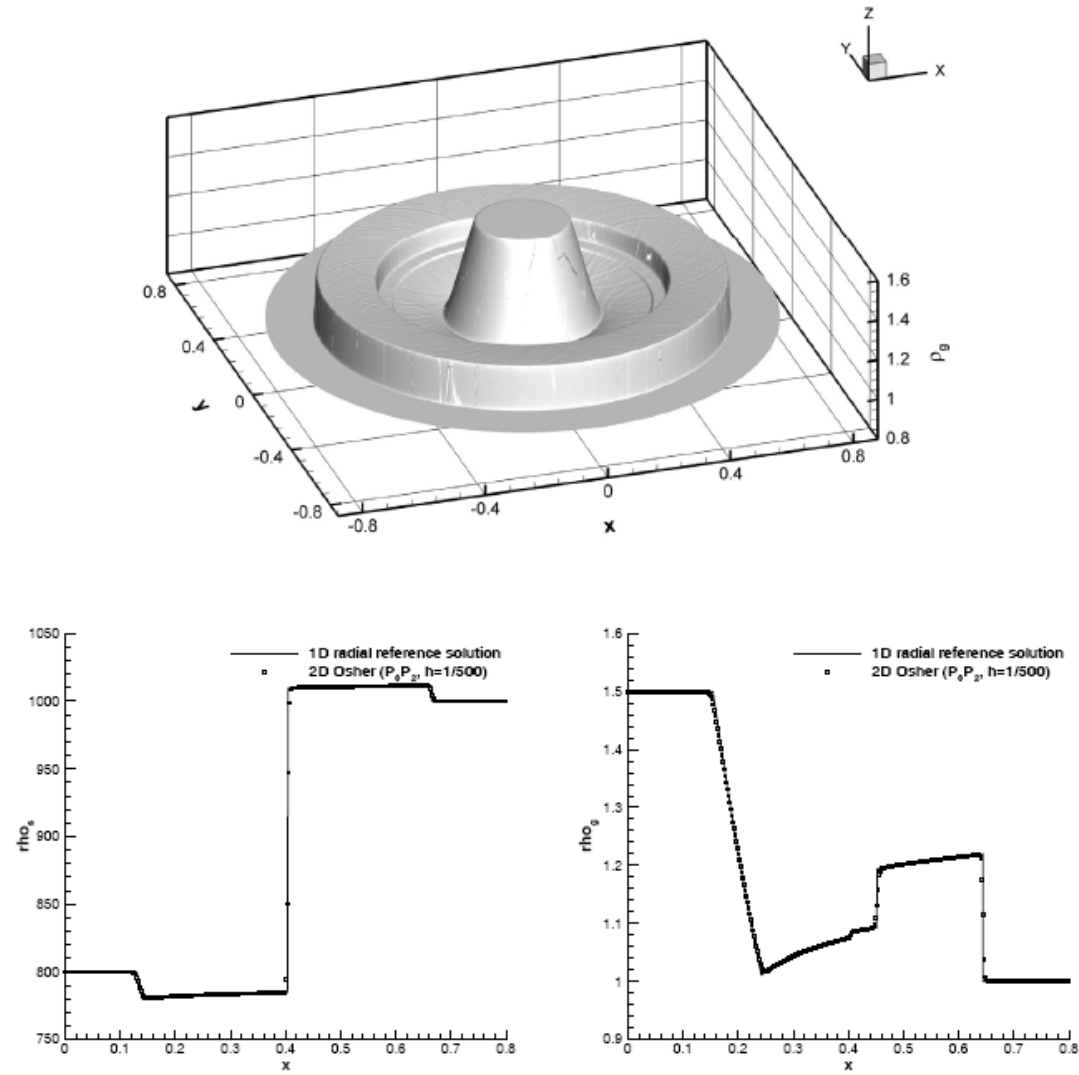
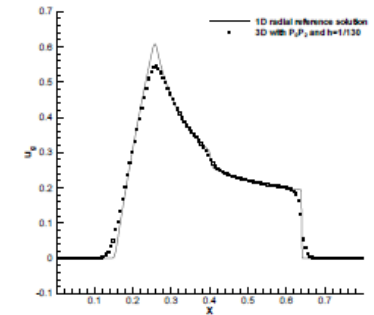
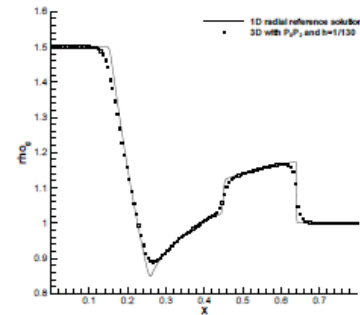
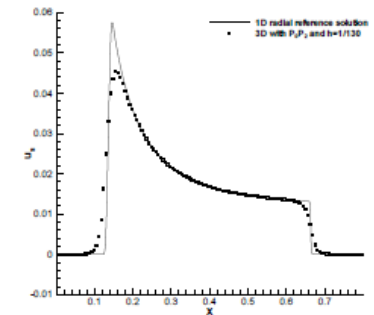
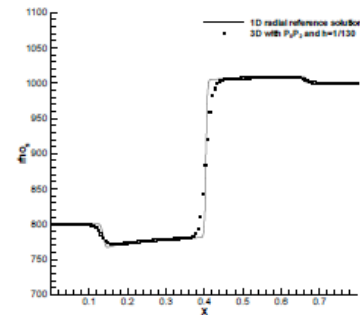
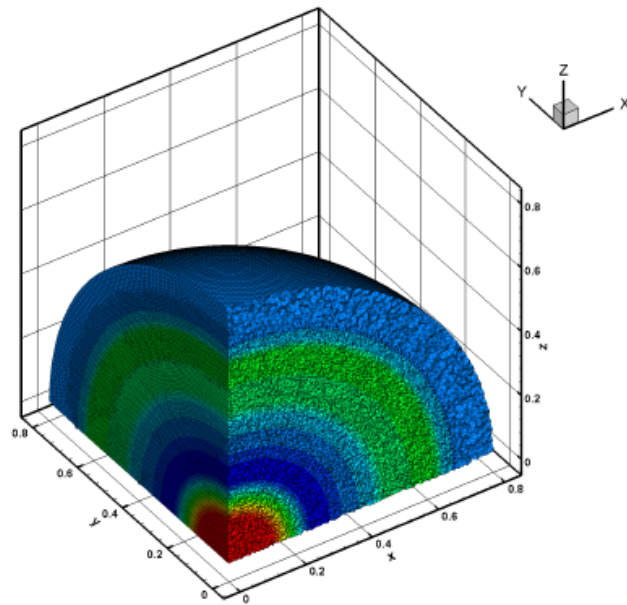
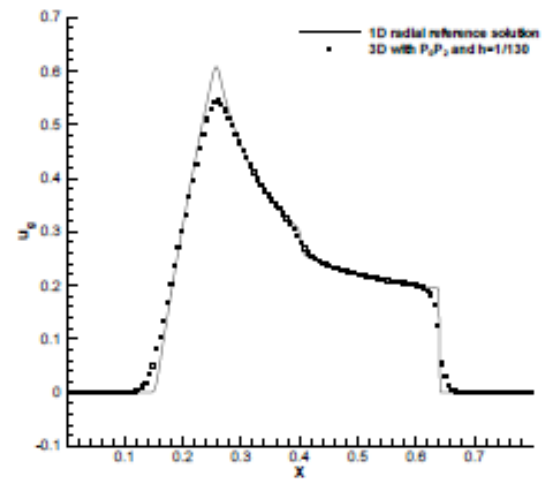
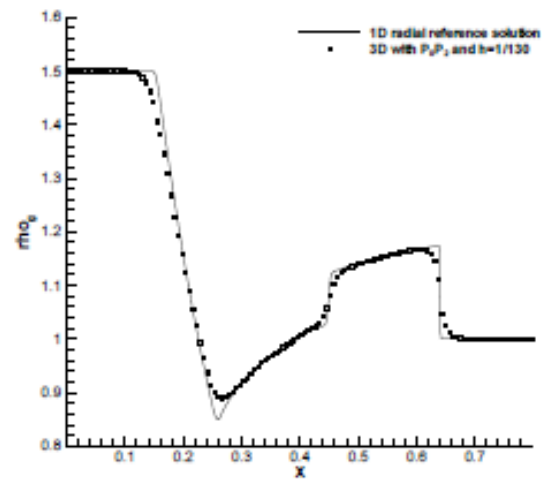
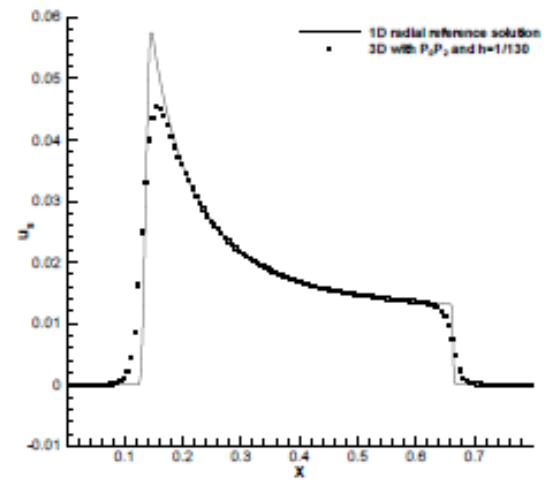
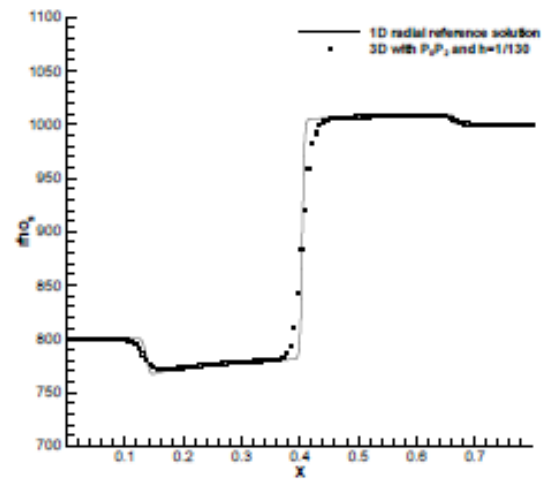


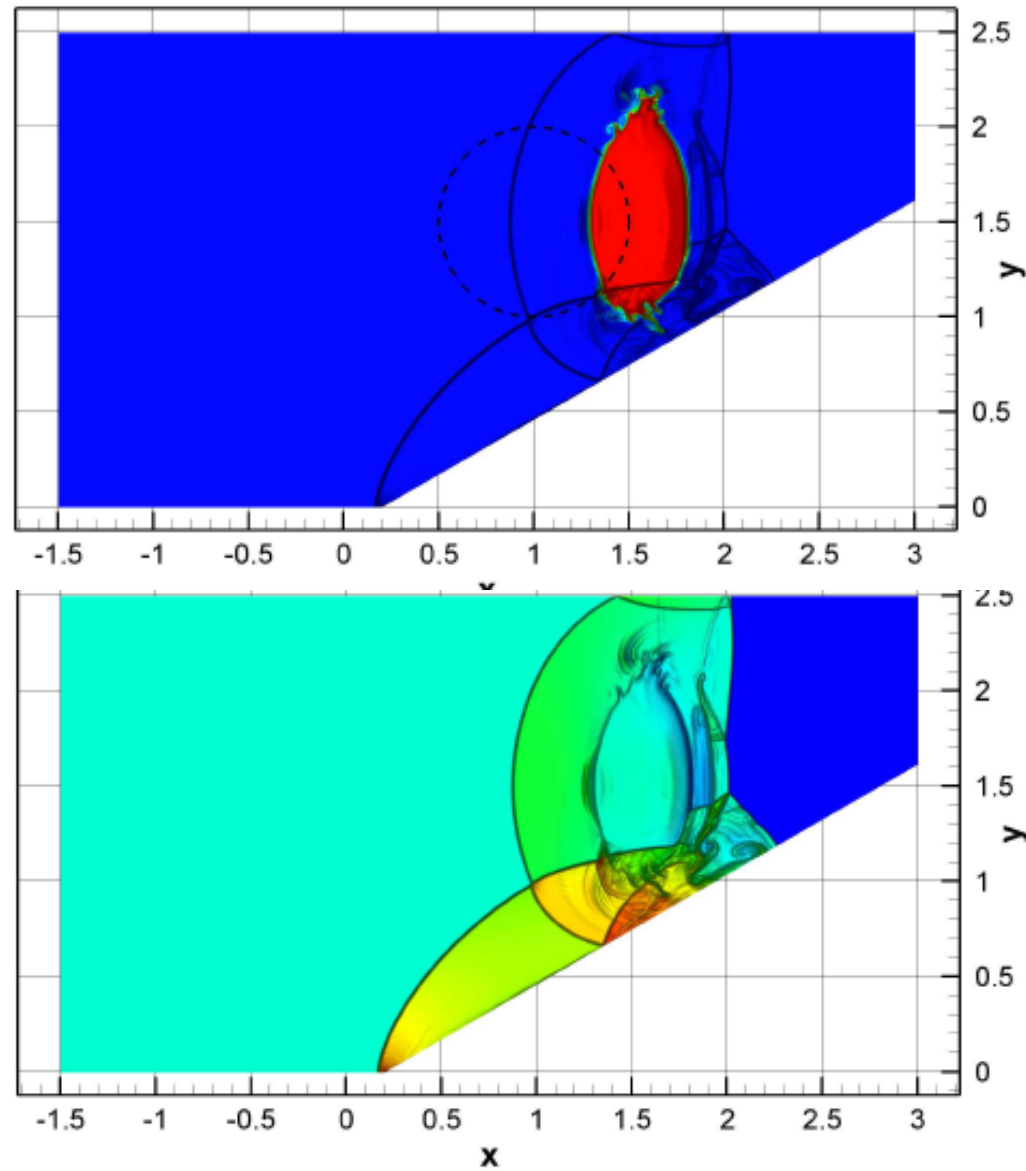
Figure 7: Results of the 2D explosion problem for the Baer–Nunziato equations at $t = 0.18$. Computational domain and 3D view of the solution (top), cuts through the solid density (left) and the gas density (right) at $y = 0$ and $t = 0.18$.

3D Baer-Nunziato equations: spherical explosion



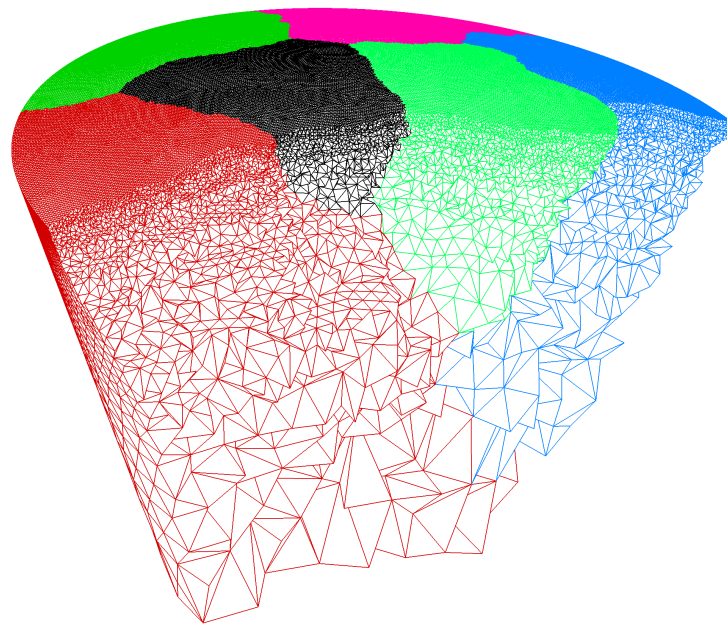
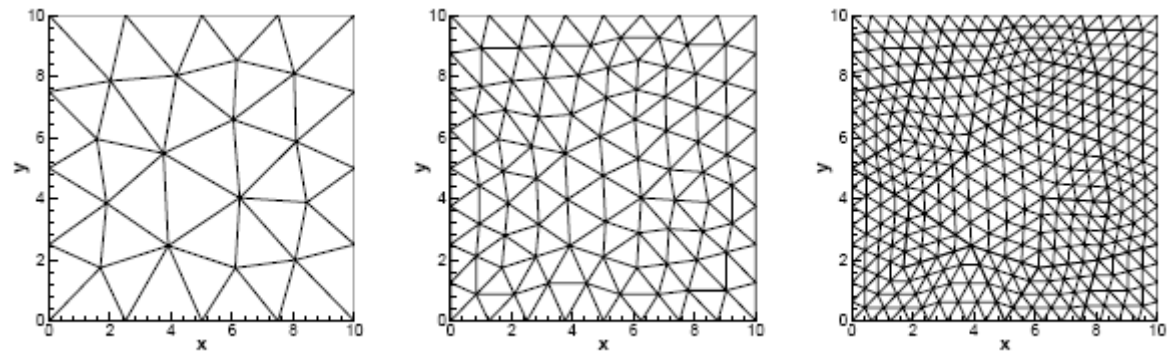


Double Mach reflection for the 2D Baer-Nunziato equations



6

Convergence rates



2D non-linear Euler equations on unstructured meshes

M. Dumbser, M. K aser, V. A. Titarev, and E. F. Toro. Quadrature-Free Non-Oscillatory Finite Volume Schemes on Unstructured Meshes for Nonlinear Hyperbolic Systems. *J. Comput. Phys.*, 226(8):204–243, 2007.

Table 4

Numerical convergence results obtained with ADER-FV schemes from third to six order in space and time for the two-dimensional vortex test case at $t = 10.0$.

$\frac{h_0}{h}$	L^∞	L^1	L^2	\mathcal{O}_{L^∞}	\mathcal{O}_{L^1}	\mathcal{O}_{L^2}	$t_{\text{CPU}}[s]$
ADER-FV $\mathcal{O}3$ (M=2)							
2	4.1966E-01	2.5803E-02	5.5744E-03				1
4	2.0603E-01	1.0377E-02	2.5127E-03	1.0	1.3	1.1	9
8	3.9381E-02	2.0124E-03	4.7131E-04	2.4	2.4	2.4	72
16	6.4677E-03	3.8149E-04	8.4719E-05	2.6	2.4	2.5	583
32	8.8072E-04	5.2530E-05	1.1666E-05	2.9	2.9	2.9	4607
ADER-FV $\mathcal{O}4$ (M=3)							
2	3.7427E-01	2.0632E-02	4.7927E-03				2
4	5.2403E-02	4.1394E-03	7.4081E-04	2.8	2.3	2.7	14
8	1.0180E-02	4.5537E-04	8.6607E-05	2.4	3.2	3.1	114
16	3.6210E-04	2.5185E-05	4.5212E-06	4.8	4.2	4.3	910
32	1.6601E-05	1.0891E-06	1.8424E-07	4.4	4.5	4.6	7188
ADER-FV $\mathcal{O}5$ (M=4)							
2	3.4130E-01	1.8162E-02	4.2424E-03				3
4	4.3610E-02	2.8756E-03	5.4369E-04	3.0	2.7	3.0	21
8	8.4151E-03	3.6375E-04	7.6764E-05	2.4	3.0	2.8	172
16	2.9109E-04	1.6616E-05	3.6625E-06	4.9	4.5	4.4	1364
32	1.0793E-05	5.7088E-07	1.3018E-07	4.8	4.9	4.8	11010
ADER-FV $\mathcal{O}6$ (M=5)							
2	2.1257E-01	1.9073E-02	2.9774E-03				3
4	3.7012E-02	2.2336E-03	3.6602E-04	2.5	3.1	3.0	32
8	1.2839E-03	9.6264E-05	1.7198E-05	4.8	4.5	4.4	261
16	3.4407E-05	1.6378E-06	3.5529E-07	5.2	5.9	5.6	2122
32	5.3451E-07	2.7486E-08	4.7517E-09	6.0	5.9	6.2	16975

Non-linear Euler equations with very stiff source terms

Table 2

Numerical convergence rates for the very stiff case ($\nu = 10^8$) obtained with ADER finite volume schemes from second to sixth order of accuracy in space and time

N_G	L^1	L^2	L^∞	\mathcal{O}_{L^1}	\mathcal{O}_{L^2}	\mathcal{O}_{L^∞}
<i>ADER-FV</i> $\mathcal{O}2$, ($M = 1$). $\nu = 10^8$						
8	2.9784E-02	3.0049E-02	3.4246E-02			
16	6.3522E-03	7.2830E-03	1.1337E-02	2.2	2.0	1.6
32	5.2567E-04	8.5936E-04	1.7792E-03	3.6	3.1	2.7
64	1.2096E-04	2.1170E-04	4.3802E-04	2.1	2.0	2.0
128	1.5717E-05	3.8232E-05	1.0892E-04	2.9	2.5	2.0
<i>ADER-FV</i> $\mathcal{O}3$, ($M = 2$). $\nu = 10^8$						
8	3.5814E-03	5.0870E-03	9.2163E-03			
16	4.5652E-04	6.7004E-04	1.2552E-03	3.0	2.9	2.9
32	5.7309E-05	8.4607E-05	1.6027E-04	3.0	3.0	3.0
64	7.1382E-06	1.0613E-05	2.0140E-05	3.0	3.0	3.0
128	8.9658E-07	1.3275E-06	2.5379E-06	3.0	3.0	3.0
<i>ADER-FV</i> $\mathcal{O}4$, ($M = 3$). $\nu = 10^8$						
4	1.4142E-02	1.9636E-02	3.8569E-02			
8	1.0485E-03	1.2385E-03	2.3951E-03	3.8	4.0	4.0
16	6.4253E-05	7.5030E-05	1.4553E-04	4.0	4.0	4.0
32	3.9752E-06	4.6373E-06	9.0331E-06	4.0	4.0	4.0
64	2.4920E-07	2.8917E-07	5.5709E-07	4.0	4.0	4.0
<i>ADER-FV</i> $\mathcal{O}5$, ($M = 4$). $\nu = 10^8$						
4	1.3054E-02	1.5158E-02	2.4062E-02			
8	4.9450E-04	6.3210E-04	1.2255E-03	4.7	4.6	4.3
16	1.6179E-05	2.1235E-05	4.3216E-05	4.9	4.9	4.8
32	5.3935E-07	6.8713E-07	1.4690E-06	4.9	4.9	4.9
64	2.0147E-08	2.5747E-08	6.4216E-08	4.7	4.7	4.5
<i>ADER-FV</i> $\mathcal{O}6$, ($M = 5$). $\nu = 10^8$						
4	8.3790E-03	9.9571E-03	2.2749E-02			
8	1.6980E-04	2.0617E-04	5.0498E-04	5.6	5.6	5.5
12	1.5336E-05	1.8986E-05	4.7918E-05	5.9	5.9	5.8
16	2.7812E-06	3.4641E-06	8.9977E-06	5.9	5.9	5.8
20	7.5301E-07	9.5840E-07	2.5566E-06	5.9	5.8	5.6

Diffusion-reaction equations

Table 9

Convergence rates for the nonlinear inhomogeneous example with restricted ENO reconstruction. Accuracy orders from 7th to 10th

ADER-RD _{7,4}						
15	0.25×10^{-3}		0.32×10^{-3}		0.66×10^{-3}	
30	0.85×10^{-6}	8.17	0.92×10^{-6}	8.43	0.14×10^{-5}	8.86
60	0.87×10^{-8}	6.62	0.98×10^{-8}	6.55	0.19×10^{-7}	6.22
120	0.79×10^{-10}	6.78	0.91×10^{-10}	6.75	0.18×10^{-9}	6.75
ADER-RD _{8,4}						
15	0.18×10^{-3}		0.22×10^{-3}		0.41×10^{-3}	
30	0.33×10^{-6}	9.09	0.40×10^{-6}	9.11	0.86×10^{-6}	8.90
60	0.15×10^{-8}	7.85	0.21×10^{-8}	7.60	0.54×10^{-8}	7.30
120	0.56×10^{-11}	8.03	0.77×10^{-11}	8.06	0.21×10^{-10}	8.03
ADER-RD _{9,5}						
15	0.98×10^{-4}		0.11×10^{-3}		0.19×10^{-3}	
30	0.50×10^{-7}	10.94	0.66×10^{-7}	10.68	0.13×10^{-6}	10.54
60	0.72×10^{-10}	9.44	0.88×10^{-10}	9.54	0.17×10^{-9}	9.52
120	0.14×10^{-12}	8.99	0.16×10^{-12}	9.08	0.27×10^{-12}	9.33
ADER-RD _{10,5}						
15	0.82×10^{-4}		0.94×10^{-4}		0.18×10^{-3}	
30	0.36×10^{-7}	11.15	0.49×10^{-7}	10.90	0.12×10^{-6}	10.60
60	0.55×10^{-10}	9.34	0.69×10^{-10}	9.48	0.16×10^{-9}	9.50
120	0.57×10^{-13}	9.92	0.73×10^{-13}	9.89	0.20×10^{-12}	9.67

E. F. Toro and A. Hidalgo. ADER Finite Volume Schemes for Diffusion–Reaction Equations.
Applied Numerical Mathematics, 59:73–100, 2009.

Convergence rates for the Baer-Nunziato equations in 2D unstructured meshes

N_G	L^2	\mathcal{O}_{L^2}	L^2	\mathcal{O}_{L^2}	L^2	\mathcal{O}_{L^2}	L^2	\mathcal{O}_{L^2}	L^2	\mathcal{O}_{L^2}	L^2	\mathcal{O}_{L^2}
$\mathcal{O}2$	P_0P_1		P_1P_1									
64/24	1.86E-01		2.04E-01									
128/48	5.94E-02	1.7	3.04E-02	2.7								
192/64	2.80E-02	1.9	1.45E-02	2.6								
256/128	1.75E-02	1.6	1.92E-03	2.9								
$\mathcal{O}3$	P_0P_2		P_1P_2		P_2P_2							
32 /16	5.09E-01		2.77E-01		5.59E-02							
64 /24	1.63E-01	1.6	8.97E-02	2.8	1.67E-02	3.0						
128/32	3.50E-02	2.2	2.91E-02	3.9	6.56E-03	3.2						
192/64	1.16E-02	2.7	2.07E-03	3.8	7.84E-04	3.1						
$\mathcal{O}4$	P_0P_3		P_1P_3		P_2P_3		P_3P_3					
32 /16	1.71E-01		1.95E-01		2.14E-02		1.77E-02					
64 /24	1.71E-02	3.3	4.95E-02	3.4	3.79E-03	4.3	2.46E-03	4.9				
128/32	1.28E-03	3.7	1.45E-02	4.3	8.95E-04	5.0	5.61E-04	5.1				
192/64	2.80E-04	3.7	5.16E-04	4.8	3.94E-05	4.5	2.07E-05	4.8				
$\mathcal{O}5$	P_0P_4		P_1P_4		P_2P_4		P_3P_4		P_4P_4			
32 /16	2.09E-01		9.85E-02		9.70E-03		5.22E-03		1.79E-03			
64 /24	2.30E-02	3.2	1.75E-02	4.3	1.18E-03	5.2	5.56E-04	5.5	2.24E-04	5.1		
128/32	1.16E-03	4.3	3.27E-03	5.8	2.09E-04	6.0	8.36E-05	6.6	4.36E-05	5.7		
192/64	1.63E-04	4.8	4.53E-05	6.2	7.23E-06	4.9	2.28E-06	5.2	1.75E-06	4.6		
$\mathcal{O}6$	P_0P_5		P_1P_5		P_2P_5		P_3P_5		P_4P_5		P_5P_5	
32 / 8	8.45E-02		5.50E-01		1.49E-01		6.22E-02		5.90E-02		2.76E-02	
64 /16	3.09E-03	4.8	8.72E-02	2.7	5.90E-03	4.7	1.73E-03	5.2	6.12E-04	6.6	4.69E-04	5.9
128/24	5.95E-05	5.7	1.46E-02	4.4	6.18E-04	5.6	1.39E-04	6.2	4.18E-05	6.6	3.72E-05	6.2
192/32	5.39E-06	5.9	2.39E-03	6.3	8.31E-05	7.0	2.17E-05	6.5	5.12E-06	7.3	4.99E-06	7.0

Michael Dumbser^{a,*}, Arturo Hidalgo^b, Manuel Castro^c, Carlos Parés^c and Eleuterio F. Toro^a *FORCE schemes on unstructured meshes II: Non-conservative hyperbolic systems* . Computer methods in Applied Science and Engineering, Vol. 199, Issues 9-12, pp 625-647, January 2010.

ADER-DG O2							
h	N_d	L^∞	L^1	L^2	O_{L^∞}	O_{L^1}	O_{L^2}
6.51	2,978	4.0950E-01	7.3710E+01	3.1185E+00			
3.26	11,913	1.7949E-01	2.1142E+01	1.0785E+00	1.2	1.8	1.5
1.63	47,653	4.4793E-02	3.9943E+00	2.2639E-01	2.0	2.4	2.3
0.81	190,610	8.2223E-03	6.3435E-01	3.7319E-02	2.4	2.7	2.6
ADER-DG O4							
h	N_d	L^∞	L^1	L^2	O_{L^∞}	O_{L^1}	O_{L^2}
13.03	2,478	1.8482E-01	3.1944E+01	1.3455E+00			
6.51	9,928	2.5445E-02	2.1268E+00	1.0901E-01	2.9	3.9	3.6
3.26	39,710	1.8028E-03	6.0709E-02	3.4818E-03	3.8	5.1	5.0
1.63	158,842	1.2070E-04	2.8285E-03	1.8062E-04	3.9	4.4	4.3
ADER-DG O6							
h	N_d	L^∞	L^1	L^2	O_{L^∞}	O_{L^1}	O_{L^2}
26.05	1,302	2.3490E-01	5.7109E+01	1.9630E+00			
13.03	5,208	2.7394E-02	4.1956E+00	1.8993E-01	3.1	3.8	3.4
6.51	20,832	9.1437E-04	4.6738E-02	2.3541E-03	4.9	6.5	6.3
3.26	83,328	1.5737E-05	1.0614E-03	5.6039E-05	5.9	5.5	5.4
ADER-DG O8							
h	N_d	L^∞	L^1	L^2	O_{L^∞}	O_{L^1}	O_{L^2}
26.05	2,232	8.3906E-02	2.3316E+01	8.4765E-01			
13.03	8,928	3.0905E-03	4.7899E-01	2.2030E-02	4.8	5.6	5.3
6.51	35,712	4.5237E-05	2.6535E-03	1.2786E-04	6.1	7.5	7.4
3.26	142,848	1.3771E-07	1.4681E-05	7.7184E-07	8.4	7.5	7.4
ADER-DG O9							
h	N_d	L^∞	L^1	L^2	O_{L^∞}	O_{L^1}	O_{L^2}
26.05	2,790	5.5839E-02	1.4153E+01	5.2238E-01			
13.03	11,160	1.0213E-03	1.6167E-01	7.4949E-03	5.8	6.5	6.1
6.51	44,640	4.6598E-06	4.9232E-04	2.5595E-05	7.8	8.4	8.2
3.26	178,560	1.7872E-08	1.3131E-06	7.0996E-08	8.0	8.6	8.5
ADER-DG O10							
h	N_d	L^∞	L^1	L^2	O_{L^∞}	O_{L^1}	O_{L^2}
26.05	3,410	3.2304E-02	8.6122E+00	3.2389E-01			
13.03	13,640	3.6709E-04	5.4707E-02	2.6230E-03	6.5	7.3	6.9
6.51	54,560	8.8532E-07	1.0717E-04	5.2679E-06	8.7	9.0	9.0
3.26	218,240	1.1050E-09	9.6184E-08	5.2430E-09	9.6	10.1	10.0

Table 20.1. ADER discontinuous Galerkin schemes. Convergence rates for schemes of second to tenth order of accuracy in space and time, as applied to the linearized Euler equations on the very irregular unstructured meshes depicted in Fig. 20.6. (Courtesy of Dr. M. Dumbser).

7

*Summary and
Concluding remarks*

- *Schemes of arbitrary accuracy in space and time for solving time-dependent PDEs (eg hyperbolic balance laws with stiff source terms) on unstructured meshes have been presented*
- *Non-linear reconstruction + generalized Riemann problem*
- *One-step, fully discrete, conservative and non-linear*
- *Unified frame, all orders in single scheme*

Schemes are well established in two important scientific communities:

Acoustics

Seismology

Important advances in:

*tsunami wave propagation
and
astrophysics*

Current work: further simplification of algorithms

Introduction to ADER approach in chapter 19 and 20:

Eleuterio Toro.

Riemann solvers and numerical methods for fluid dynamics.

A practical introduction.

Third edition. Springer-Verlag, Berlin Heidelberg, 2009.

Book (724 pages). ISBN 978-3-540-25202- 3, 2009.

Thank you